**Proceedings of IMECE2005**
**2005 ASME International Mechanical Engineering Congress and Exposition**
**November 5-11, 2005, Orlando, Florida USA**

**IMECE2005-82633**

# A MULTI-FINGERED MICROMECHANISM FOR COORDINATED MICRO/NANO MANIPULATION

**Sandeep Krishnan**
*Graduate Student*

**Laxman Saggere**
*Assistant Professor*

Micro- Systems Mechanisms and Actuators Laboratory
Department of Mechanical and Industrial Engineering
University of Illinois at Chicago, Chicago, IL, 60605 USA

## ABSTRACT

Micromanipulators for coordinated manipulation of micro- and nano-scale objects are critical for advancing several emerging applications such as microassembly and manipulation of biological cells. Most of existing designs for micromanipulators accomplish either primarily microgripping or primarily micropositioning tasks, and relatively, only a very few are capable of accomplishing both microgripping and micropositioning, however, they are generally bulky.

This paper presents conceptualization, design, fabrication and experimental characterization a novel micromanipulation station for coordinated planar manipulation combining both gripping and positioning of micro- and nano-scale objects. Conceptually, the micromanipulation station is comprised of multiple, independently actuated, fingers capable of coordinating with each other to accomplish the manipulation and assembly of micron-scale objects within a small workspace. A baseline design is accomplished through a systematic design optimization of each finger maximizing the workspace area of the manipulation station using the optimization toolbox in MATLAB. The device is micromachined on a SOI (silicon-on-insulator) wafer using the DRIE (Deep Reactive Ion Etching) process. The device prototype is experimentally characterized for the output displacement characteristics of each finger for known input displacements applied through manual probing. An excellent correlation between the experimental results and the theoretical results obtained through a finite element analysis in ANSYS software, which validates both the design and the fabrication of the proof-of-the-concept, is demonstrated.

**Keywords** Micromanipulation, Microgripper, Microposition, Micromechanism.

## INTRODUCTION

Micromanipulation typically involves two major tasks: microgripping, i.e., gripping of objects at micro-scale, and micropositioning, i.e., pick-and-place of micro-scale objects with high degree of accuracy. Such micromanipulation involving both tasks is essential to advance emerging MEMS applications such as assembly of microfabricated components in microfactories and manipulation of biological cells in bio-mechanotransduction studies. Accomplishment of advanced manipulation tasks involving both microgripping and micropositioning in many of these applications demand coordinated motion of multiple grippers and manipulators.

Many different designs and tools for accomplishing manipulation at micro/nano-scales have been developed or proposed in the literature. Most of these micromanipulators are designed to accomplish either primarily microgripping or primarily micropositioning, and relatively, only a very few are designed for accomplishing both microgripping and micropositioning simultaneously. Manipulator devices developed primarily for gripping function include the pickup-and-release device utilizing pressure variations based on temperature changes inside micro-holes [1], the electrostatically driven microgripper [2], individually actuated fingers comprising piezoelectrically bending unimorphs [3]. Other grippers in this category include [4], [5], and [6].

Manipulator devices that primarily accomplish micropositioning functionality include the following: the 6-degree-of-freedom (DOF) micropositioning stage based on magnetic levitation principles [7], a rigid 6-DOF parallel platform for precision 3-D micromanipulation utilizing pressurized deformable cylinders as micro-actuators [8], a 3-DOF parallel micromechanisms utilizing flexure hinges [9], a

parallel manipulator articulated with five revolute type flexure joints [10], and a multi-DOF device comprising soft gel actuator elements for soft micromanipulation [11]. Other devices in this category include micropositioners [12] and [13].

The devices that attempt to combine both gripping and micropositoning tasks include the following: Chopstick manipulator [14] that is capable of manipulating micro-scale objects in 3 dimensions, the MINIMAN, a piezo-ceramic bimorph actuated locomotive robot on which probes can be mounted [15], [16], positioning stages with end magnetically-driven effectors that physically push mechanical parts to carry out assembly [17], a micro-hand for the dexterous manipulation of small mechanical parts and biological objects [18], and a micro-robot that integrates a microgripper with a piezo positioning stage [19]. The chopstick model [14] can be considered as an example of macro-scale mechanisms that operate in the micro-domain, and hence unsuitable for large-scale operations involving coordination between manipulators and complex maneuvers with high dexterity. Micro-scale manipulators that are created by integrating microgrippers with positioning stages require further assembly after fabrication in order to realize the device.

The above literature survey reveals lack of a compact device with combined gripping and positioning functionalities for coordinated micromanipulation. This paper concerns the development of a new design, called the micromanipulation station, for such functionality. The following sections describe the concept, design methodology, fabrication, and experimental characterization of the new device.

## CONCEPT

Conceptually the micromanipulation station is a miniaturized, monolithic (single-piece) compliant mechanism with multiple *fingers*. Figure 1 shows a specific instance of this concept featuring four fingers arranged orthogonally. Each finger can interact with every other finger and all fingers are independently controlled. Each *finger* in the manipulation station is comprises of a *pincher* that directly interacts with an object and a *body* that modifies and transmits the input displacements to the tip of the pincher or *fingertip*. Each finger is actuated by two inputs, located symmetrically about the pincher, at the base of the *body* (see Fig. 2). The input to each finger is either a displacement or force at each actuation point and the output is the displacement at the fingertip. The finger can move with equal propensity on either side of the pincher. The range of motion of all the fingertips defines the *workspace* of the manipulation station. Multiple modes of potential coordination between the fingers are illustrated in Fig. 3. The overall size of the device is 1 cm × 1 cm. The device is designed to be able to manipulate objects of sizes about 5–10 μm.

In this concept, an aspect of which is illustrated in Fig.1 is designed to accomplish coordinated gripping, 2-D positioning and rotation of objects in the workspace. The rotation can be accomplished by relative x-y positioning of the fingertips. Independent motion of fingers in the device leads to increased flexibility of operation by imparting a high degree of rotary freedom to an object held between fingers.

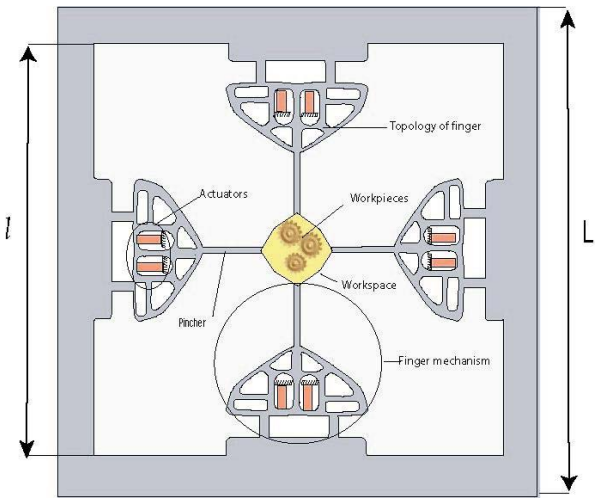


**Fig. 1 Schematic of the micromanipulation station.**

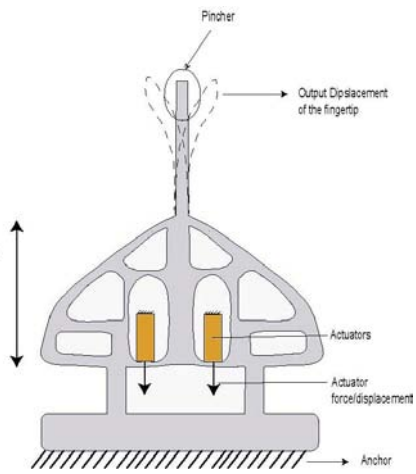


**Fig. 2 Component details of a finger in the micromanipulation station.**

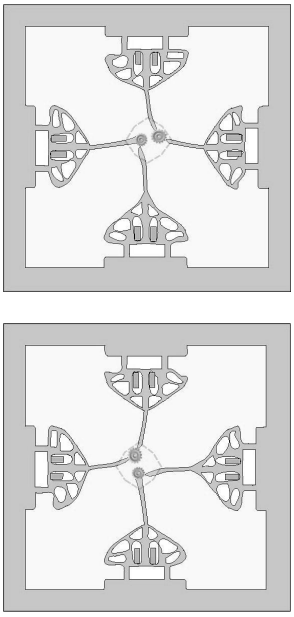

**Fig. 3 Manipulation possibilities.**

## DESIGN

### Design problem statement

A baseline design has been obtained through a systematic design approach, involving optimization of the topology and dimensions of the manipulator with the objective of maximizing the workspace of the manipulation station for a given set of input displacements and associated constraints.

The design strategy involves the following steps:

i. Choose an appropriate *ground structure* to represent the initial topology of the design optimization problem.
ii. Obtain a mathematical function that describes the effective workspace of the manipulation station. This function serves as the objective function for the design optimization.
iii. Identify the constraints that define the boundaries for the design domain.
iv. Pose design problem as a min/max optimization criterion.

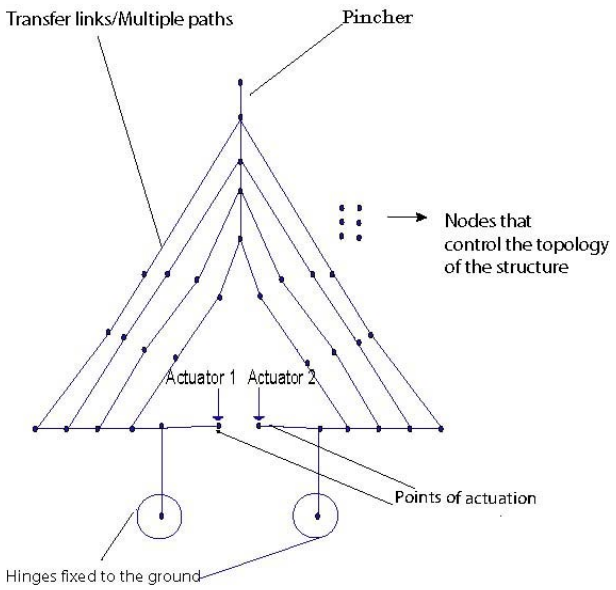


**Fig. 4 A potential *ground structure* topology for the design optimization of each finger of the manipulation station.**

The initial topology or the *ground structure* for the design optimization problem is selected in a way to enhance the mechanical advantage of the mechanism (ratio of output displacement at fingertip to input displacement at actuator) as shown in the line diagram in Fig. 4. The figure shows the finger anchored at two locations with the two inputs (displacement or force) applied in the plane of the finger symmetrically with respect to the pincher tip. The basis for selection of this particular *ground structure* is the lever principle that amplifies input displacements by pivoting the mechanism about the anchor points. For the current base-line design, 4 fingers are chosen and arranged as shown in Fig. 1.

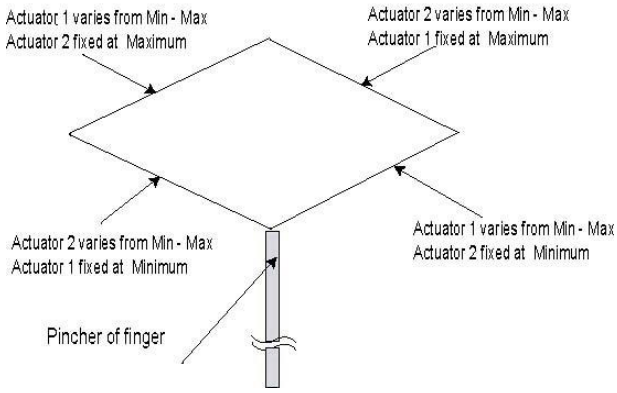


**Fig. 5 Workspace boundaries.**

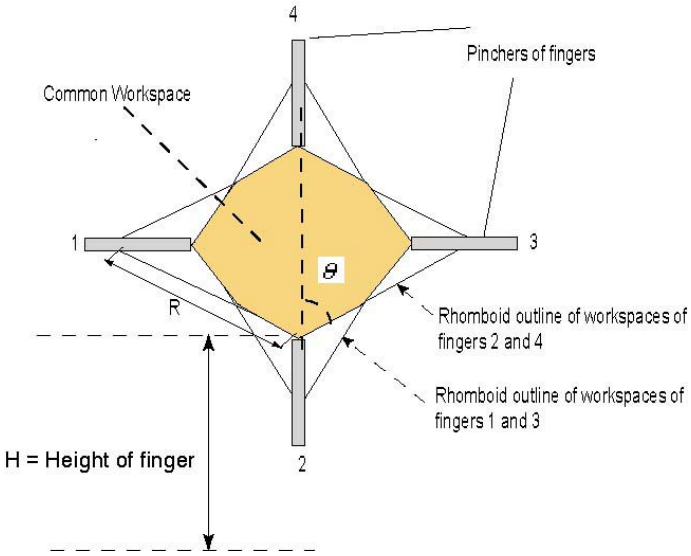


**Fig. 6 Common workspace for all fingers.**

The objective function which is defined as the Effective workspace of the manipulation station is given by

$$W_e = W_c - W_o ,$$

where,

$W_e$ = Effective workspace for coordinated manipulation,
$W_c$ = Common workspace for all fingers
$W_o$ = Portion of the common workspace in which gripping and coordination cannot occur due to its distortion

The free workspace of each finger for a specified input actuation displacement range is plotted assuming a linear response of the finger and is a rhombus as shown in Fig.5. The common workspace $W_c$ as shown in Fig. 6 is the overlap of free workspaces of individual fingers. The effective workspace is distorted as a result of gripping forces as shown in Fig. 7. The distortion $W_o$ is negligible for the typical order of the forces involved in the design considered. Hence, the maximization of $W_e$ is effectively the same as maximizing $W_c$.

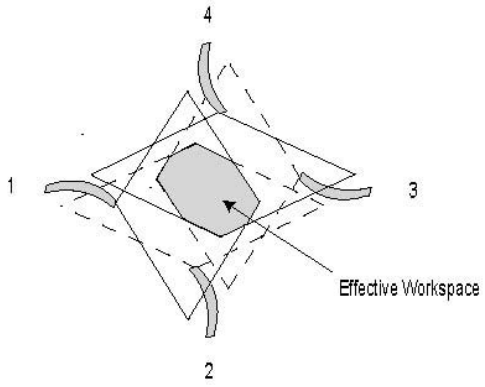


**Fig. 7 Postgripping effective workspace.**

The Common workspace is given by:

1. For $\theta \le (\pi/4)$

$$W_C = 4 \cdot R^2 \cdot \frac{(\sin\theta)^2 . \cos(\theta)}{\sin(\theta) + \cos(\theta)}; \quad (1)$$

2. For $\theta \ge (\pi/4)$

$$W_C = 4 \cdot R^2 \cdot \frac{(\cos\theta)^2 . \sin(\theta)}{\sin(\theta) + \cos(\theta)}; \quad (2)$$

where,

$R$ = Length of rhombus side (Fig. 6)
$\theta$ = Angle shown in Fig. 6.

The design constraints define the boundaries or limits of the design domain. The actuators are constrained to operate in a range of 0-10 μm in displacement output. The design space for the overall dimensions of each finger is restricted to a rectangle of boundaries 4mm × 5mm. The dimension '*l*' for the manipulation station (Fig. 1) is constrained and not allowed to exceed 8 mm. This limit is imposed to restrict the total size ($L$ x $L$) of the manipulation station to about 1 cm × 1 cm. The parameter '*l*' is given by: $l = 2 \cdot (H + R\cos\theta)$, where $H$ is the height of a finger (Fig. 6).

Since an actuator is not actually chosen for integration into the manipulation station, an upper limit of 30 mN is imposed on the maximum force that it can exert. The actuators are assumed to be fixed to the mechanism at the actuation points thus preventing any horizontal or vertical motion of the structure at these points, other than the motion caused due to actuator input itself.

Finally using the above objective function and constraints, the design problem is posed as:

$$Maximize \quad W_C \quad (3)$$

Subject to equilibrium equations and boundary conditions (as consistent with Fig. 4) and,

Actuator range = 0-10 μm (4)

$l \le 8\ mm$ (5)

$Input\ force\ of\ actuator \le 30\ mN$ (6)

Bounded design space = 4mm × 5mm rectangle (7)

## Design Optimization Implementation

The design optimization was implemented and solved as outlined below:

i. Creation of a finite element (FE) model of initial ground topology, and
ii. Optimization of the ground structure for the design problem posed in the previous section.

A finite element model of the *ground topology* was created in MATLAB environment. The finger is modeled using a frame structure and uses beam elements to model solid connections. The connectivity of these elements is fixed and represents the *ground structure* shown in Fig. 4. The locations, orientations and thicknesses of the beam elements in the frame model define the topology of the structure. Control nodes shown in Fig. 4 define the position and orientation of these beam elements. The space coordinates of the control nodes and the thicknesses of elements that connect these nodes constitute the design variable vector - $\bar{x}$. The symmetry of the finger is exploited to reduce the number of design variables. The FE program computes $W_c$ as a function of $\bar{x}$ and the constraints imposed on the model.

The design inputs to the FE code are also the design variables in the optimization model. The optimization toolbox in MATLAB is used to set up and carry out the design optimization. Optimization is carried out using the non-linear constrained optimization function *fmincon*, which uses a Sequential Quadratic Programming (SQP) method to obtain optimal solutions. In order to prevent any unacceptable crossing of links and drive the solution away from infeasibile geometries, geometric constraints were imposed in the FE code. The initial solution to the optimization routine is a simplified representation of the *ground structure* discussed in the previous section. For the preliminary design, only one of the potential multiple paths in the ground structure shown in Fig. 4 is made active at a time so that only one path connects the actuation input and fingertip, and other paths are made inactive by assigning near zero thickness. Figure 8 illustrates the chosen initial topology whose shape and size are variable. Table 1 shows the initial values and bounds on the widths applied to the elements that constitute the design domain. The two links that anchor the finger to the outer frame are called *anchor links*.

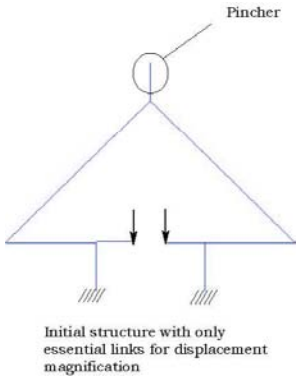


**Fig. 8 Initial topology for the design optimization.**

**Table 1 Initial values and bounds applied on thickness of links in design domain.**

| | Thickness | | |
|---|---|---|---|
| | **Initial value (μm)** | **Lower bound (μm)** | **Upper bound (μm)** |
| Anchor links | 60 | 50 | 300 |
| Active links | 100 | 100 | 300 |

The lower limits on the anchoring links are kept at 50 μm from structural strength considerations. The out of plane thickness of the structure is fixed to be uniformly 20 μm. The thickness of the *pincher* portion of the finger is kept constant throughout optimization at 10 μm. Constraints represented in Eqs. (4) – (6) are imposed on the design optimization routine. Upper and lower bounds are imposed on the node locations consistent with Eq. (7).

## Optimization Results

The results of the MATLAB optimization are detailed in this section. The overall size and structure of the optimized finger structure are shown in Fig. 9. Width of links in the optimized shape varied from 52.9 μm to 284.87 μm.

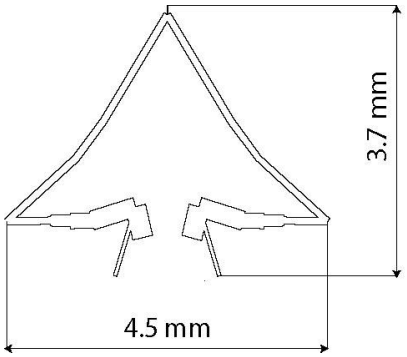


**Fig. 9 Optimized shape of the finger.**

The height and width of each finger are 3.7 mm and 4.5 mm respectively. The widths of links in the optimized topology vary between 52.9 μm and 284.87 μm. The results of optimization and their comparison with the initial structure are shown in Table 2. The results show a considerable improvement in the objective function in the optimized solution. The common workspace $W_c$ increased from 85.97 $\mu m^2$ in the initial solution to 2500 $\mu m^2$ in the optimized solution.

**Table 2 Comparison of Initial and Optimized solutions.**

| | **Initial solution** | **Optimal solution** |
|---|---|---|
| R (μm) | 13.44 | 59.34 |
| θ | $65.37^0$ | $57.33^0$ |
| Common Workspace, $W_c$ ($\mu m^2$) | 85.97 | 2500 |
| Actuator force (mN) | 10.83 | 30 |

In order to validate the MATLAB results and visualize the finger motion behavior, the initial and final optimized solutions are also modeled as solid models in ANSYS. The plane frame representation in MATLAB is compared with an equivalent solid model in ANSYS for both initial and optimized solutions (Fig. 10 & 11, Tables 3 & 4). PLANE82 elements are used to model the finger in ANSYS. The comparison of the results listed in Tables 3 & 4 shows a very good agreement between the MATLAB and ANSYS models, thus validating the FE code implemented in MATLAB.

**Table 3 Comparison of results for initial solutions in MATLAB and ANSYS.**

| | **MATLAB initial sol.** | **ANSYS solid model** |
|---|---|---|
| R (μm) | 13.44 | 13.76 |
| θ | $65.37^0$ | $65.10^0$ |
| Common Workspace- $W_c$ ($\mu m^2$) | 85.97 | 91.68 |
| Actuator force (mN) | 10.83 | 9.87 |

**Table 4 Comparison of results of optimized solution in MATLAB and ANSYS.**

| | **MATLAB Optimized** | **ANSYS Solid Model** |
|---|---|---|
| R (μm) | 59.34 | 57.088 |
| θ | $57.33^0$ | $58.84^0$ |
| Common Workspace, $W_c$ ($\mu m^2$) | 2500 | 2175.3 |
| Actuator force (mN) | 30 | 37.72 |

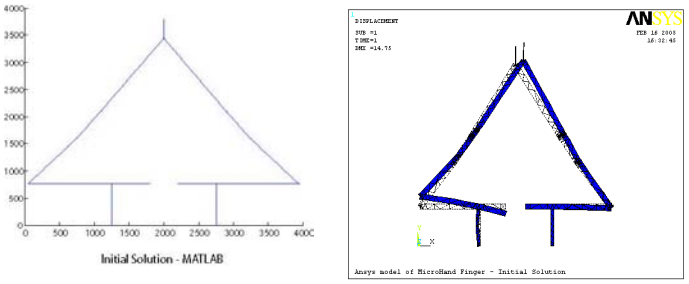


**Fig. 10 Initial solutions in MATLAB (left) and ANSYS (right).**

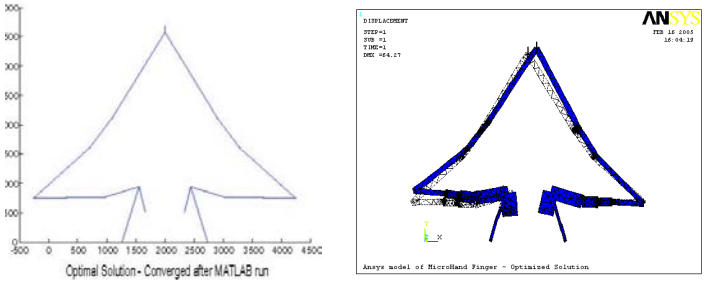


**Fig. 11 Optimal Solutions in MATLAB (left) and ANSYS (right).**

Figure 12 shows the workspace of fingers obtained from the ANSYS model of the optimized solution. F1 and F2 are the actuation forces of actuators 1 and 2 respectively. The actuator force at maximum displacement of actuator of 10 µm is found to be 37.72 mN in the ANSYS model. The optimized solution is modified to include notches near the actuation points to facilitate mechanical probing of the structure.

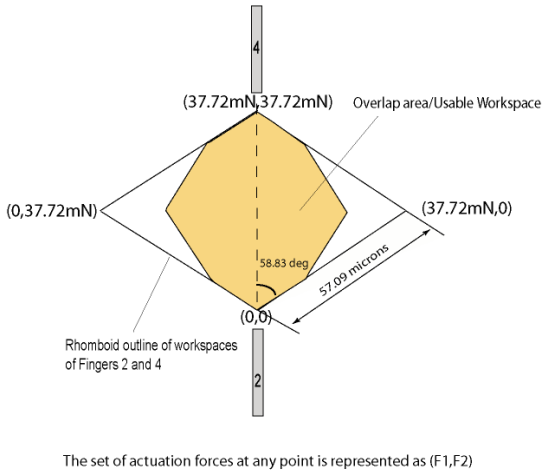


**Fig. 12 Optimized common workspace model.**

## FABRICATION

The device was fabricated on an SOI (silicon-on-insulator) wafer, which had a device layer thickness of 20 µm, buried oxide layer thickness of 2 µm and handle layer thickness of 250 µm. The microfabrication process sequence is illustrated in Fig. 13 and briefly described below.

Photololithography was carried out on the wafer followed by Deep Reactive Ion Etching (DRIE) for 5 minutes. This ensured that the silicon was etched all the way through 20 µm down to the oxide. The etch rate of DRIE on silicon dioxide is considerably lower than that of silicon and hence the oxide layer serves effectively as an etch stop. The wafer was then diced into small dies of 1 $cm^2$ each. The finger structure was then released in 49% concentrated HF after immersion for 83 minutes.

A picture of the die is shown in Fig. 14(A and B). A high degree of stiction was observed between the device and the substrate on many of the dies. To produce a stiction-free prototype for experimentation, the 20 µm-thick device side layer was completely separated from the handle side by etching away the oxide layer in 49% HF for several hours and then attached to a plastic holder with an 8 mm × 8 mm recess to facilitate the mechanical characterization. The device was then actuated using 125 µm diameter probe tips mounted on precise micropositioners as described in the following section.

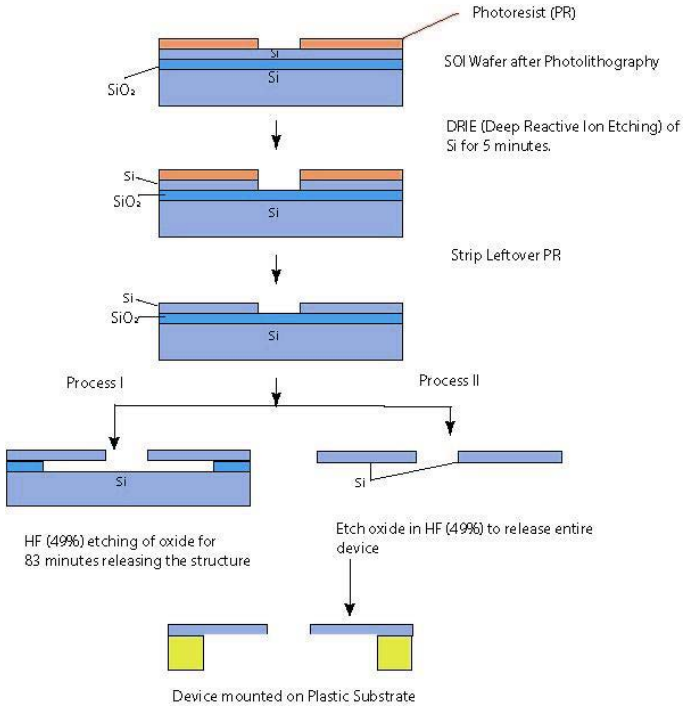

**Fig. 13 Process flow for device micromachining.**

using a microscope and a camera attached to a computer. The experimental setup is shown in Fig. 15.

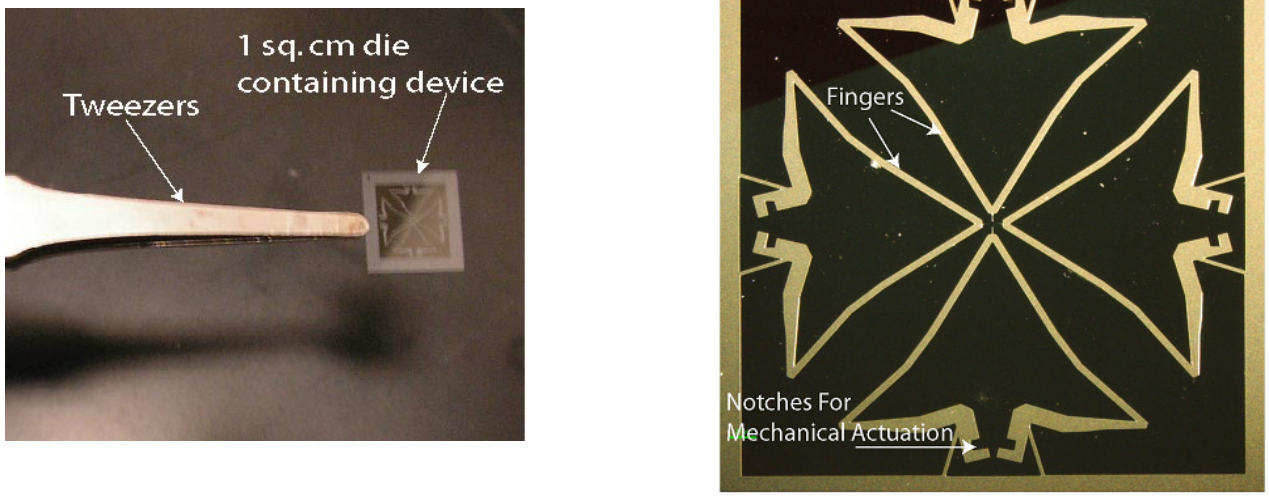


**Fig. 14 Device held by tweezers (A), Device close up using a stereo Microscope (B).**

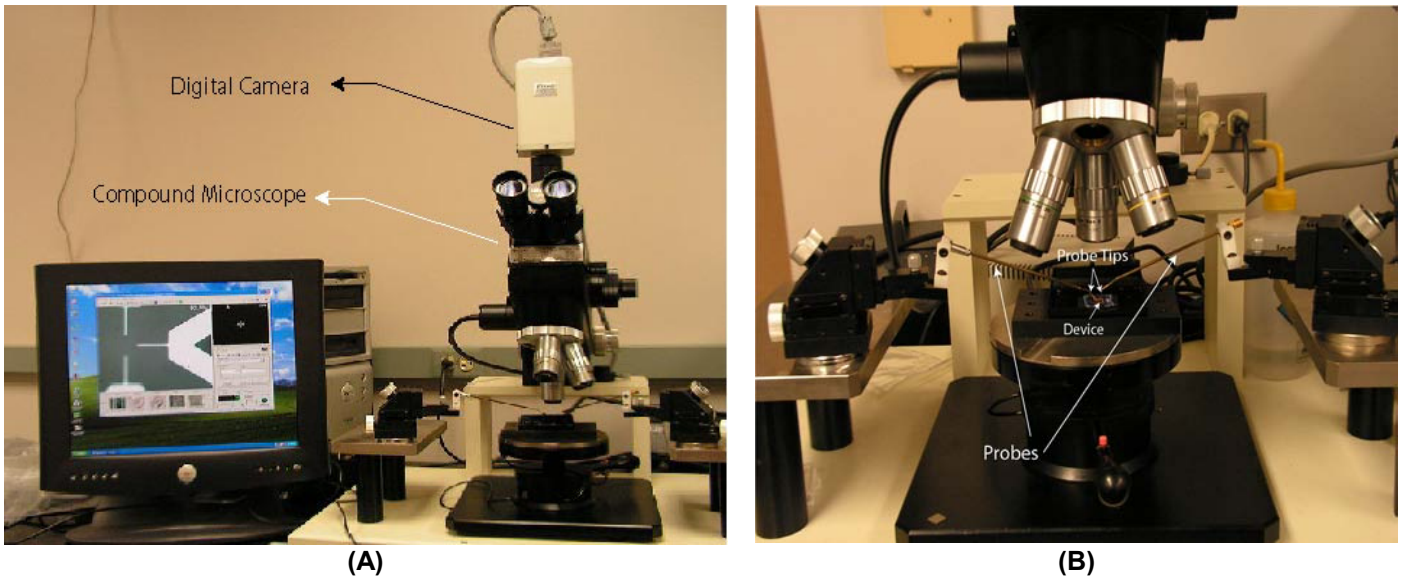


**Fig. 15 Experimental setup for mechanical probing (A), Close-up of the setup (B).**

## EXPERIMENT

The purpose of experimentation is to verify the mechanical behavior of the fabricated finger mechanism by measuring its input actuation to output displacement characteristics. The output measured is the tip displacement, which is captured

The device was placed in a gel box to prevent any bulk motion during actuation. Only one of the two nodes of actuation on each finger was actuated. The other node was left unconstrained. Probes mounted on manual micropositioners are maneuvered to pull down on the notches at the input nodes to provide actuation in the form of displacement to the finger. The

displacements are measured on a calibrated image acquired through Nikon DMX-1200 digital camera and ACT-1 software. Both the input actuation and the fingertip motion were tracked as part of measurement. The close-up details of the input actuation and the output finger response are shown in Fig. 16.

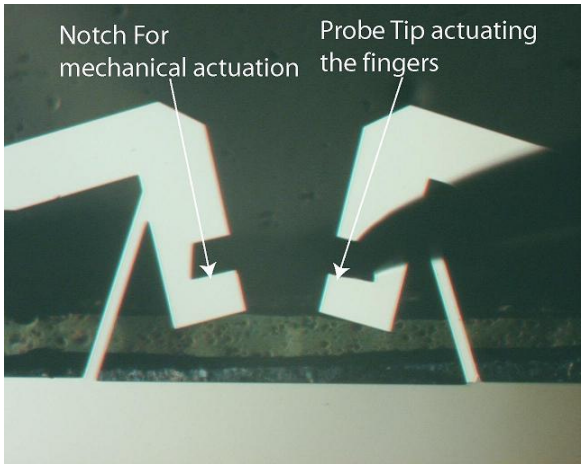


**(A) Probe Tip actuating structure.**

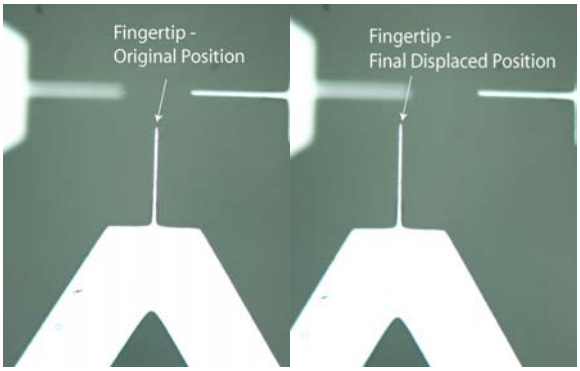


**(B) Finger tip response.**

**Fig. 16 Close-up details of the input actuation and the output fingertip response motion tracking.**

The *x* and *y* displacements of the fingertip were measured for increasing input displacement. In order to characterize device response and compare the same with finite element analysis results, a single finger under the same boundary conditions was modeled in ANSYS. The experimental readings were compared with a set of values obtained from the ANSYS model and were found to have excellent correlation. The results are summarized in Table 5 and Fig. 17.

**Table 5 Numerical comparison of experimental and theoretical results.**

| Input Actuation (μm) | ANSYS Output | | Expt. Output | |
|---|---|---|---|---|
| | X (μm) | Y (μm) | X (μm) | Y (μm) |
| 0 | 0 | 0 | 0 | 0 |
| 3 | 25.75 | 2.17 | 30 | 2 |
| 5 | 42.92 | 3.61 | 47 | 4 |
| 7 | 60.09 | 5.06 | 60 | 6 |
| 9 | 77.25 | 6.50 | 73 | 7.5 |
| 11 | 94.42 | 7.95 | 92 | 10 |

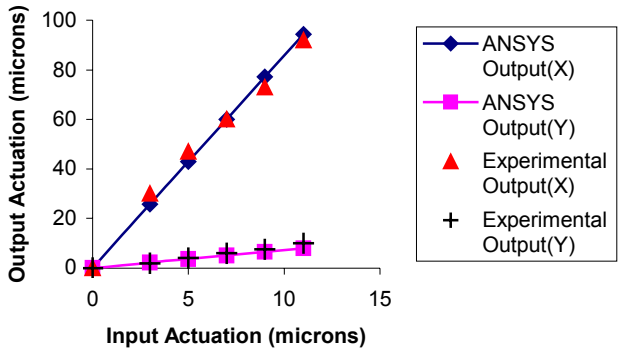


**Fig. 17 Graphical comparison of experimental and theoretical output.**

## CONCLUSION

A novel concept for planar coordinated micromanipulation is presented and a baseline design of the concept obtained through systematic topology optimization for maximization of the workspace is fabricated and characterized. The excellent correlation demonstrated between the experimental and theoretical results of the input/output characteristics of a finger of a proof-of-the-concept manipulator station validates the theoretical design principles and the fabrication process.

The first-generation proof-of-concept manipulator station presented in this work was designed for applying the inputs by manual probing for simplicity. As such, coordinated manipulation was not demonstrated in this manipulator station due to limited control of the finger motion achievable with manual probing. However, the future generation devices currently under development will incorporate tiny piezoelectric actuators as input sources for each finger. Incorporation of these actuators for inputs would lend greater degree of control over the finger mechanism's motion, and thus, enable coordinated manipulation with multiple fingers.

## REFERENCES


[1] Arai, F., and Fukuda, T., "A new pick up and release method by heating for micromanipulation," *Proceedings, IEEE., Tenth Annual International Workshop on Micro Electro Mechanical Systems,* 1997, pp. 383-388.

[2] Kim, C.-., Pisano, A.P., and Muller, R.S., "Overhung electrostatic microgripper," *Solid-State Sensors and Actuators, Digest of Technical Papers,* 1991, pp. 610-613.

[3] Haddab, Y., Chaillet, N., and Bourjault, A., "A microgripper using smart piezoelectric actuators," *Proceedings. IEEE/RSJ International Conference on Intelligent Robots and Systems,* Vol. 1, 2000, pp. 659-664 vol.1.

[4] Kohl, M., Krevet, B., and Just, E., "SMA microgripper system," *Transducers, Eurosensors XV,* Vol. 97-98, Elsevier Science B.V, Munich, 2002, pp. 646-652.

[5] Thornell, G., Bexell, M., and Schweitz, J.-., "Design and fabrication of a gripping tool for micromanipulation," *Proc. of the 8th International Conference on Solid-State Sensors and Actuators, and Eurosensors IX. Part 2 (of 2),* Vol. 2, IEEE, Piscataway, NJ, USA, Stockholm, Sweden, 1995, pp. 388-391.

[6] Carrozza, M.C., Menciassi, A., and Tiezzi, G., "The development of a LIGA-microfabricated gripper for micromanipulation tasks," *Journal of Micromechanics and Microengineering,* Vol. 8, No. 2, 1998, pp. 141-3.

[7] Jung, K.S., and Baek, Y.S., "Contact-free moving-magnet type of micropositioner with optimized specification," *IEEE Transactions on Magnetics,* Vol. 38, No. 3, 2002, pp. 1539-1548.

[8] Portman, V.T., Sandler, B.-., and Zahavi, E., "Rigid 6-DOF parallel platform for precision 3-D micromanipulation," *International Journal of Machine Tools and Manufacture,* Vol. 41, No. 9, 2001, pp. 1229-1250.

[9] Yi, B.-., Chung, G.B., and Na, H.Y., "Design and experiment of a 3-DOF parallel micromechanism utilizing flexure hinges," *IEEE Transactions on Robotics and Automation,* Vol. 19, No. 4, 2003, pp. 604-612.

[10] Alici, G., and Shirinzadeh, B., "Description and kinematic analysis of a planar micromanipulation system based on flexure joints," *Proc. International Conference on Advanced Intelligent Mechatronics,* Vol. 2, 2003, pp. 1274-1279.

[11] Tadokoro, S., Yamagami, S., and Ozawa, M., "Multi-DOF device for soft micromanipulation consisting of soft gel actuator elements," *Proceedings. IEEE International Conference on Robotics and Automation,* Vol. 3, 1999, pp. 2177-2182.

[12] Chang, S.H., Tseng, C.K., and Chien, H.C., "An ultra-precision XY&thetas;$_Z$ piezo-micropositioner. I. Design and analysis," *IEEE Transactions on Ultrasonics, Ferroelectrics and Frequency Control,* Vol. 46, No. 4, 1999, pp. 897-905.

[13] Chang, S.H., Tseng, C.K., and Chien, H.C., "An ultra-precision XYΘ$_Z$ piezo-micropositioner. II. Experiment and performance," *IEEE Transactions on Ultrasonics, Ferroelectrics and Frequency Control,* Vol. 46, No. 4, 1999, pp. 906-912.

[14] Tanikawa, T., and Arai, T., "Development of a micro-manipulation system having a two-fingered micro-hand," *IEEE Transactions on Robotics and Automation,* Vol. 15, No. 1, 1999, pp. 152-62.

[15] Lopez-Sanchez, J., Simu, U., and Puig-Vidal, M., "A miniature robot driven by smart power integrated circuits," *IEEE/RSJ International Conference on Intelligent Robots and Systems,* Vol. 2, Institute of Electrical and Electronics Engineers Inc, Lausanne, Switzerland, 2002, pp. 1954-1959.

[16] Lopez-Sanchez, J., Miribel-Catala, P., and Montane, E., "High accuracy piezoelectric-based microrobot for biomedical applications," *8th International Conference on Emerging Technologies and Factory Automation,* Vol. 2, Institute of Electrical and Electronics Engineers Inc, Antibes-Juan les pins, 2001, pp. 603-609.

[17] Inoue, T., Hamasaki, Y., and Shimoyama, I., "Micromanipulation using a microcoil array," *Proceedings., IEEE International Conference on Robotics and Automation,* Vol. 3, 1996, pp. 2208-2213.

[18] Nakamura, T., Kogure, Y., and Shimamura, K., "A micro operation hand and its application to microdrawing," *Proceedings. IEEE International Conference on Robotics and Automation,* Vol. 2, IEEE, San Francisco, CA, USA, 2000, pp. 1095-100.

[19] Ferreira, A., Agnus, J., and Chaillet, N., "A smart microrobot on chip: Design, identification, and control," *IEEE/ASME Transactions on Mechatronics,* Vol. 9, No. 3, 2004, pp. 508-519.